Novel Rotor-Flux Observer Using Observer Characteristic Function in Complex Vector Space for Field-Oriented Induction Motor Drives

Jang-Hwan Kim, *Student Member, IEEE*, Jong-Woo Choi, *Member, IEEE*, and Seung-Ki Sul, *Fellow, IEEE*

***Abstract*—This paper proposes a new strategy to estimate the rotor flux of an induction machine. The electrical model of the induction machine presents the basic idea based on an observer structure, which is composed of a voltage model and a current model. However, the former has the defects of sensitivity to machine parameters in the low-speed range, and the latter also has defects that are sensitive to the machine parameters in wide-speed range. In spite of these shortcomings, the closed-loop flux observer based on two models has been a prevalent estimation method for direct field-oriented control. In this paper, a generalized analysis method called the "observer characteristic function method" is proposed to analyze all kinds of the linear flux observers in an unified form. By the observer characteristic function being utilized, the estimated rotor-flux error involved in the classical methods can be easily clarified. Moreover, the novel rotor-flux observer based on this analysis is also presented. The proposed flux observer is robust to the offset voltage and to parameter variation. The effectiveness of the novel flux observer has been verified by the numerical analysis and experimental results.**

***Index Terms*—Field-oriented control, flux observer, induction machines, observer characteristic function.**

NOMENCLATURE

$\mathbf{v_s}$	Stator voltage (V).
$\mathbf{i_s}$	Stator current (A).
$\boldsymbol{\lambda}_\mathbf{s}^\mathbf{s}$	Stator flux in stationary reference frame (Wb).
$\boldsymbol{\lambda}_\mathbf{r}^\mathbf{s}$	Rotor flux in stationary reference frame (Wb).
ω_e	Synchronous angular speed (rad/s).
ω_r	Rotor angular speed (rad/s).
ω_{sl}	Slip frequency (rad/s).
r_s, r_r	Stator resistance and rotor resistance (Ω).
L_s, L_r	Stator inductance and rotor inductance (H).
L_m	Mutual inductance (H).
L_{ls}, L_{lr}	Stator leakage inductance and rotor leakage inductance (H).
$p = d/dt$	Derivative operator.

Paper IPCSD 02–023, presented at the 2001 Applied Power Electronics Conference, Anaheim, CA, March 4–8, and approved for publication in the IEEE TRANSACTIONS ON INDUSTRY APPLICATIONS by the Industrial Drives Committee of the IEEE Industry Applications Society. Manuscript submitted for review September 5, 2001 and released for publication May 30, 2002.

J.-H. Kim and S.-K. Sul are with the School of Electrical Engineering, Seoul National University, Seoul, Korea 151-742 (e-mail: ghks95@eepel.snu.ac.kr; sulsk@plaza.snu.ac.kr).

J.-W. Choi is with the School of Electronics and Electrical Engineering, Kyungpook National University, Taegu, Korea 702-842 (e-mail: cjw@knu.ac.kr).

Publisher Item Identifier 10.1109/TIA.2002.802994.

I. INTRODUCTION

THE methods based upon a voltage and a current models are the traditional methods to estimate the rotor flux of an induction machine. Their benefits and drawbacks are well known. At high speed, the voltage model provides an accurate stator-flux estimate because the machine back electromotive force (EMF) dominates the measured terminal voltage. However, at low speeds, voltage drop across stator resistance in the stator voltage equation becomes significant, causing the accuracy of the flux estimate to be sensitive to the accuracy of estimated stator resistance and voltage measurement. Due to that sensitivity and inherent signal-integration problems at low excitation frequency, the direct field-oriented control systems based solely upon the voltage model are generally not capable of achieving high dynamic performance at low and zero speed. The current model can be an alternative to the voltage model at low and zero speed [1]. However, the current model would be expected to have the sensitivity to the rotor time constant and magnetizing inductance. The voltage model and current model are useful at nominal and low speeds, respectively. Many closed-loop flux observers utilizing the desirable low-speed attributes of the current model and the desirable high-speed attributes of the voltage model have been proposed [2]–[8].

In this paper, a generalized analysis method called the "observer characteristic function method" is proposed to analyze all kinds of the linear flux observers in an unified form. By the observer characteristic function being manipulated, the estimated flux error caused by the voltage offset and current offset and by the variation of machine parameters has been analyzed. Furthermore, the estimated rotor-flux error involved in the classical methods can be easily clarified. Finally, the novel rotor-flux observer based on this analysis is also presented. The effectiveness of the proposed flux observer has been verified by numerical analysis and experimental results.

II. FLUX OBSERVERS

The analysis of observers for an induction machine can be simplified considerably by the use of complex vector notation. The complex quantities used in this paper are written in the form $\mathbf{f}^s = f_d^s + jf_q^s$ and the superscripts $\hat{}$ denote estimated quantities.

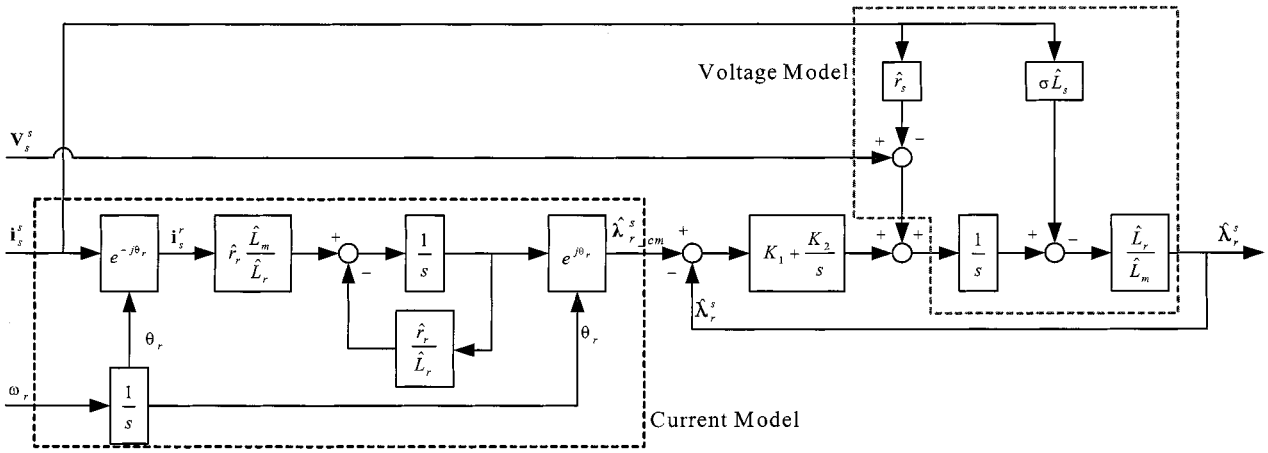

Fig. 1. Closed-loop improved Gopinath model flux observer.

A. Voltage-Model Flux Observer [2], [4]

The voltage model utilizes the stator voltages and currents, but not the rotor speed. It is commonly used to implement direct field orientation without the rotor speed feedback. From the stator voltage equation, the stator flux can be estimated by the integration of the following equation:

$$p\hat{\boldsymbol{\lambda}}_{\mathbf{s}}^{\mathbf{s}} = \mathbf{v}_s^s - \hat{r}_s \mathbf{i}_s^s \tag{1}$$

from which the rotor flux is then obtained by

$$\hat{\boldsymbol{\lambda}}_{\mathbf{r}}^{\mathbf{s}} = \frac{\hat{L}_r}{\hat{L}_m}\left(\hat{\boldsymbol{\lambda}}_{\mathbf{s}}^{\mathbf{s}} - \sigma\hat{L}_s \mathbf{i}_s^s\right). \tag{2}$$

B. Current-Model Flux Observer [1], [2]

From an induction motor electrical dynamics, the governing equation of the open-loop rotor-flux observer is as follows:

$$p\hat{\boldsymbol{\lambda}}_{\mathbf{r}}^{\mathbf{s}} = -\left(\frac{\hat{r}_r}{\hat{L}_r} - j\omega_r\right)\hat{\boldsymbol{\lambda}}_{\mathbf{r}}^{\mathbf{s}} + \hat{r}_r\frac{\hat{L}_m}{\hat{L}_r}\mathbf{i}_s^s. \tag{3}$$

The current model can also be implemented as a linear system in the rotor reference frame.

C. Improved Gopinath Model [2], [3]

The closed-loop flux observer is shown in Fig. 1 and is seen to provide an automatic transition between the two most desirable open-loop flux observer models, i.e., from the current model at low frequency to the voltage model at high frequency. The transition is now determined via the bandwidth of the flux loop.

D. Full-Order Flux Observer [5]

From the induction motor electrical model, the state space equations of full-order observer, which estimates both the stator current and rotor flux, has the form shown in (4) [5]. Equation (4) can be expressed as (5) and (6) using the complex vectors

$$p\begin{bmatrix}\hat{\mathbf{i}}_{\mathbf{s}}\\ \hat{\boldsymbol{\lambda}}_{\mathbf{r}}^{\mathbf{s}}\end{bmatrix} = \mathbf{A}\begin{bmatrix}\hat{\mathbf{i}}_{\mathbf{s}}\\ \hat{\boldsymbol{\lambda}}_{\mathbf{r}}^{\mathbf{s}}\end{bmatrix} + \mathbf{B}\mathbf{v}_{\mathbf{s}} + \mathbf{G}\left(\hat{\mathbf{i}}_{\mathbf{s}} - \mathbf{i}_{\mathbf{s}}\right) \tag{4}$$

$$p\hat{\mathbf{i}}_{\mathbf{s}} = -\frac{1}{\sigma\hat{L}_s}\left(\hat{r}_s + \hat{r}_r\frac{\hat{L}_m^2}{\hat{L}_r^2}\right)\hat{\mathbf{i}}_{\mathbf{s}} + \frac{\hat{L}_m}{\sigma\hat{L}_s\hat{L}_r}\left(\frac{\hat{r}_r}{\hat{L}_r} - j\omega_r\right)\hat{\boldsymbol{\lambda}}_{\mathbf{r}}^{\mathbf{s}} + \frac{1}{\sigma\hat{L}_s}\mathbf{v}_{\mathbf{s}} + (g_1 + jg_2)\left(\hat{\mathbf{i}}_{\mathbf{s}} - \mathbf{i}_{\mathbf{s}}\right) \tag{5}$$

$$p\hat{\boldsymbol{\lambda}}_{\mathbf{r}}^{\mathbf{s}} = \hat{r}_r\frac{\hat{L}_m}{\hat{L}_r}\hat{\mathbf{i}}_{\mathbf{s}} - \left(\frac{\hat{r}_r}{\hat{L}_r} - j\omega_r\right)\hat{\boldsymbol{\lambda}}_{\mathbf{r}}^{\mathbf{s}} + (g_3 + jg_4)\left(\hat{\mathbf{i}}_{\mathbf{s}} - \mathbf{i}_{\mathbf{s}}\right) \tag{6}$$

where $\mathbf{A}$ and $\mathbf{B}$ are the matrices containing the information of plant, $\mathbf{G}$ is the gain matrix, and $g_1 + jg_2$, $g_3 + jg_4$ are complex gain vectors [5].

E. Reduced-Order Flux Observer [7]

In the full-order observer, all the stator currents and rotor flux are estimated. However, since the stator currents are already measured, only the rotor flux should be estimated. Therefore, many researchers have studied reduced-order observers. The particular reduced-order flux observer is written as (7). The state equation (7) can be expressed as (8) and (9) using the complex vectors

$$p\begin{bmatrix}\hat{\mathbf{i}}_{\mathbf{s}}\\ \hat{\boldsymbol{\lambda}}_{\mathbf{r}}\end{bmatrix} = \mathbf{A}\begin{bmatrix}\mathbf{i}_{\mathbf{s}}\\ \hat{\boldsymbol{\lambda}}_{\mathbf{r}}\end{bmatrix} + \mathbf{B}\mathbf{v}_{\mathbf{s}} + \mathbf{G}\left(p\mathbf{i}_{\mathbf{s}} - p\hat{\mathbf{i}}_{\mathbf{s}}\right) \tag{7}$$

$$p\hat{\mathbf{i}}_{\mathbf{s}} = -\frac{1}{\sigma\hat{L}_s}\left(\hat{r}_s + \hat{r}_r\frac{\hat{L}_m^2}{\hat{L}_r^2}\right)\mathbf{i}_{\mathbf{s}} + \frac{1}{\sigma\hat{L}_s}\mathbf{v}_{\mathbf{s}} + \frac{\hat{L}_m}{\sigma\hat{L}_s\hat{L}_r}\left(\frac{\hat{r}_r}{\hat{L}_r} - j\omega_r\right)\hat{\boldsymbol{\lambda}}_{\mathbf{r}}^{\mathbf{s}} \tag{8}$$

$$p\hat{\boldsymbol{\lambda}}_{\mathbf{r}}^{\mathbf{s}} = \hat{r}_r\frac{\hat{L}_m}{\hat{L}_r}\mathbf{i}_{\mathbf{s}} - \left(\frac{\hat{r}_r}{\hat{L}_r} - j\omega_r\right)\hat{\boldsymbol{\lambda}}_{\mathbf{r}}^{\mathbf{s}} + (g_{r1} + jg_{r2})\left(p\mathbf{i}_{\mathbf{s}} - p\hat{\mathbf{i}}_{\mathbf{s}}\right) \tag{9}$$

where $\mathbf{A}$ and $\mathbf{B}$ are the matrices containing the information of plant, $\mathbf{G}$ is the gain matrix, and $g_{r1} + jg_{r2}$ is the complex gain vector [7].

III. Observer Characteristic Function

A general form for all of the linear flux observers can be described by (10) as follows, which is the combination form of

TABLE I
OBSERVER CHARACTERISTIC FUNCTIONS
($K_p = K_1\hat{L}_r/\hat{L}_m$, $K_i = K_2\hat{L}_r/\hat{L}_m$)

Observer	Observer Characteristic Function, $F(s)$
Voltage Model	1
Current Model	0
Improved Gopinath Model	$\frac{s^2}{s^2+K_p s+K_i}$
Full Order Observer	$\frac{C_2 s}{s^2+C_1 s+C_0}$
Reduced Order Observer	$\frac{C_4 s}{s+C_3}$

voltage model and current model, where $F(s)$ will be referred to as an "observer characteristic function":

$$\hat{\boldsymbol{\lambda}}^{\mathbf{s}}_{\mathbf{r}} = F(s)\left(\hat{\boldsymbol{\lambda}}^{\mathbf{s}}_{\mathbf{r\_vm}} - \hat{\boldsymbol{\lambda}}^{\mathbf{s}}_{\mathbf{r\_cm}}\right) + \hat{\boldsymbol{\lambda}}^{\mathbf{s}}_{\mathbf{r\_cm}} = F(s)\hat{\boldsymbol{\lambda}}^{\mathbf{s}}_{\mathbf{r\_vm}} + \left(1 - F(s)\right)\hat{\boldsymbol{\lambda}}^{\mathbf{s}}_{\mathbf{r\_cm}} \tag{10}$$

where $\hat{\boldsymbol{\lambda}}^{\mathbf{s}}_{\mathbf{r\_cm}}$ is the estimated rotor flux from the current model and $\hat{\boldsymbol{\lambda}}^{\mathbf{s}}_{\mathbf{r\_vm}}$ is the estimated rotor flux from the voltage model.

The observer characteristic functions of all linear flux observers can be summarized as Table I with some manipulation where C_0, C_1, C_2, and C_3 are the complex numbers to variant with the rotor speed ω_r. In the low-speed range, all the linear observers using both current and voltage models assume that the real rotor flux exists in the neighborhood of estimated rotor flux from the current model because $F(s)$ is nearly zero in the low-speed range. Similarly, in the high-speed range, all the linear observers estimate the rotor flux in the neighborhood of estimated rotor flux from the voltage model because $F(s)$ is nearly unity in the high-speed range. To estimate the rotor flux in the mid-speed range, careful attention should be taken. The possible best choice would be to assume that the rotor flux exists on the line connecting the estimated flux from the current model to the estimated flux from the voltage model, as shown in Fig. 2.

IV. ANALYSIS OF FLUX OBSERVER USING OBSERVER CHARACTERISTIC FUNCTION

In case of the proposed in [2], the estimated rotor flux can be expressed as follows:

$$\hat{\boldsymbol{\lambda}}^{\mathbf{s}}_{\mathbf{r}} = F(s)\left(\hat{\boldsymbol{\lambda}}^{\mathbf{s}}_{\mathbf{r\_vm}} - \hat{\boldsymbol{\lambda}}^{\mathbf{s}}_{\mathbf{r\_cm}}\right) + \hat{\boldsymbol{\lambda}}^{\mathbf{s}}_{\mathbf{r\_cm}} \tag{11}$$

where

$$F(s) = \frac{s^2}{s^2 + K_p s + K_i}.$$

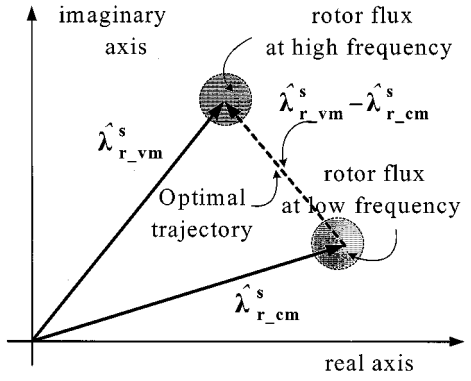

Fig. 2. Optimal estimation trajectory.

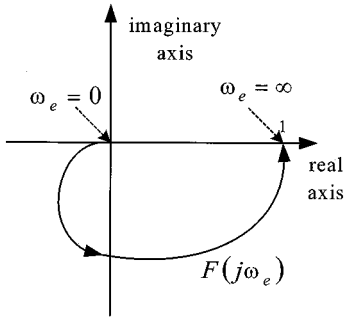

Fig. 3. FRF of the observer characteristic function in (11).

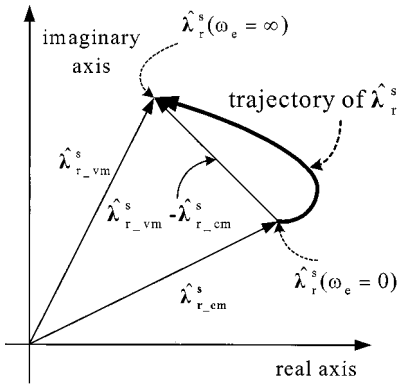

Fig. 4. Trajectory of estimated rotor flux in case of the improved Gopinath model.

At the steady state, the frequency-response function (FRF) of the observer characteristic function is as follows and as depicted in Fig. 3:

$$F(j\omega_e) = \frac{\omega_e^2}{\sqrt{(K_i - \omega_e^2)^2 + (K_p\omega_e)^2}}\, e^{j(\pi - \tan^{-1}(K_p\omega_e/K_i - \omega_e^2))}. \tag{12}$$

Thus, the estimated rotor-flux trajectory according to the synchronous angular frequency can be determined by (12) and as shown in Fig. 4. In Fig. 4, it is easily seen that the estimated rotor-flux trajectory is far from the optimal estimation trajectory shown in Fig. 2, especially in the mid-speed range. Thus, the performance of the improved Gopinath model would be much deteriorated in case of parameter error and measurement error

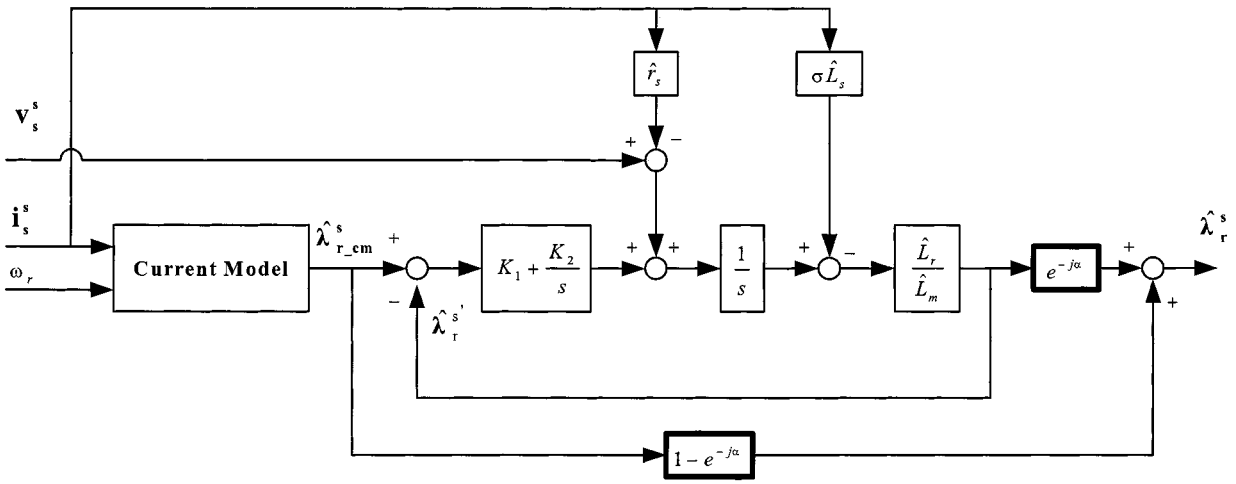

Fig. 5. Closed-loop proposed novel flux observer.

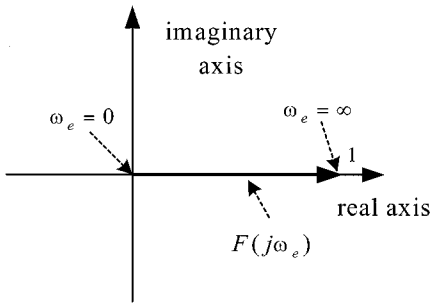

Fig. 6. FRF of the observer characteristic function in (14).

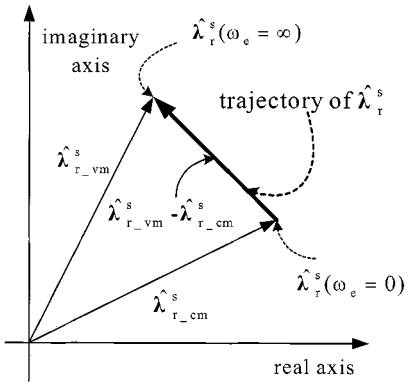

Fig. 7. Trajectory of the estimated rotor flux in case of the proposed flux observer.

in the mid-frequency region. Similarly, the other linear flux observers can be analyzed and also have the similar problems as the improved Gopinath model.

V. Proposed Flux Observer

The block diagram of the proposed flux observer is shown in Fig. 5, which adds an angle compensation block to the improved Gopinath model. The observer characteristic function of the proposed observer is given as follows:

$$F(s) = \frac{s^2}{s^2 + K_p s + K_i} e^{-j\alpha} \tag{13}$$

where

$$\alpha = \left(\pi - \tan^{-1}\left(\frac{K_p \omega_e}{K_i - \omega_e^2}\right)\right).$$

In (13), α is the angle of observer characteristic functions of the improved Gopinath model. The FRF of the observer characteristic function is as follows and as depicted in Fig. 6. Note that $F(j\omega_e)$ lies only on the real axis as follows:

$$F(j\omega_e) = \frac{\omega_e^2}{\sqrt{(K_i - \omega_e^2)^2 + (K_p\omega_e)^2}} e^{j0}. \tag{14}$$

Note that the estimated rotor-flux trajectory in Fig. 7 is much improved compared to the one in Fig. 4.

TABLE II
22-kW Induction Motor Parameters (ω_c: The Transition Frequency is Set to 6 Hz)

220V, 60Hz, 4poles			
r_r	0.0252 Ω	r_s	0.044 Ω
L_m	12.9 mH	L_{lr}	0.47 mH
L_{ls}	0.55 mH	ω_c	37.7 (rad/s)

VI. Effects of Offset Voltage and Current

Under the condition that the offset voltage and offset current exist in the pulsewidth modulation (PWM) inverter system, the effects can be analyzed by using the observer characteristic function such as shown in (15). $\Delta\boldsymbol{\lambda}^{\mathbf{s}}_{\mathbf{r\_vm}}$ and $\Delta\boldsymbol{\lambda}^{\mathbf{s}}_{\mathbf{r\_cm}}$ are the flux errors due to voltage and current offset in case of the voltage model and current model, respectively. The steady-state error can be easily evaluated by the final value theorem

$$\Delta\boldsymbol{\lambda}^{\mathbf{s}}_{\mathbf{r}} = \lim_{s\to 0} s\Big(F(s)\Delta\boldsymbol{\lambda}^{\mathbf{s}}_{\mathbf{r\_vm}} + \big(1 - F(s)\big)\Delta\boldsymbol{\lambda}^{\mathbf{s}}_{\mathbf{r\_cm}}\Big) \tag{15}$$

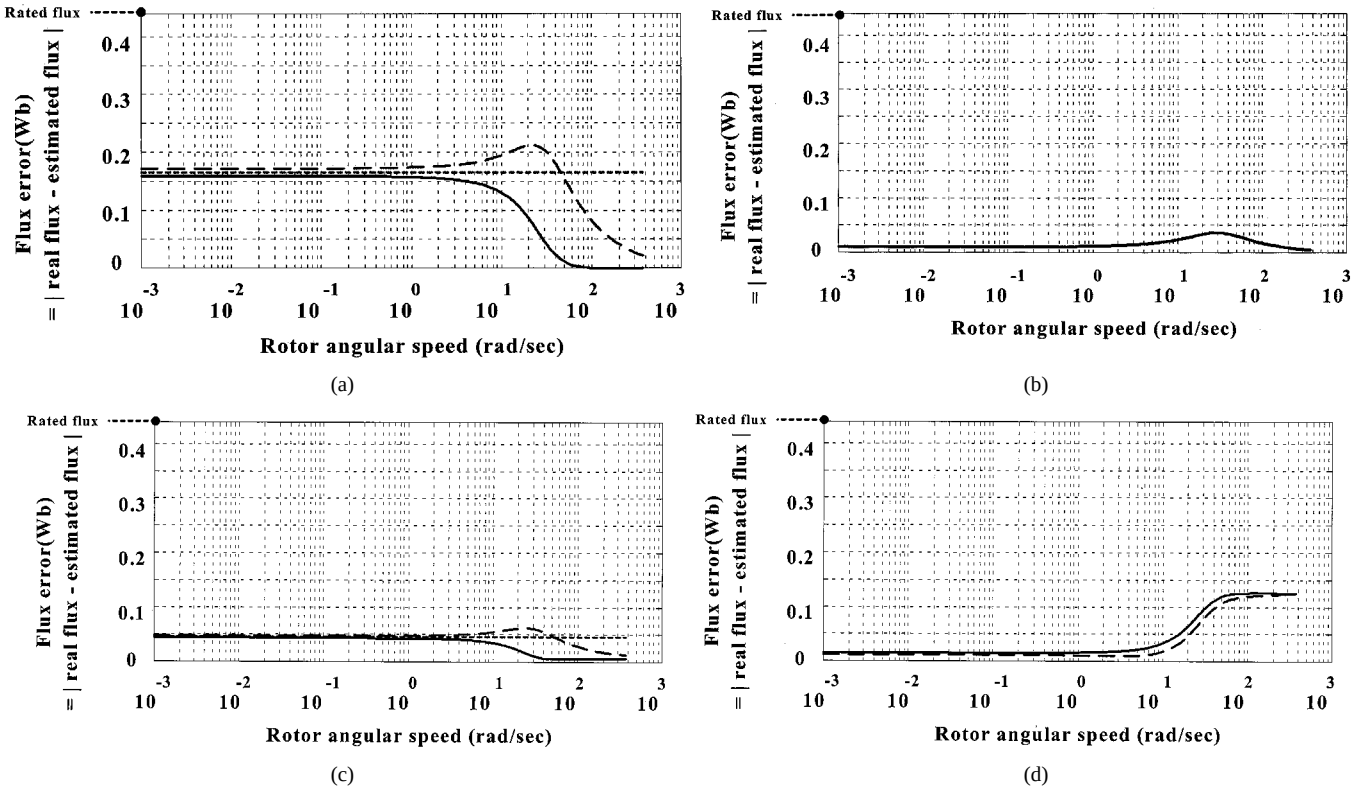

Fig. 8. Numerical analysis: flux errors of the flux observer at rated slip. (a) $\hat{r}_r = 1.4r_r$ case (flat dotted line is the flux error of current model). (b) $\hat{r}_s = 1.3r_s$ case. (c) $\hat{L}_m = 0.7L_m$ case (flat dotted line is the flux error of the current model). (d) $\hat{\sigma}\hat{L}_s = 1.9\sigma L_s$ case. (Solid line: proposed case; dotted line: improved Gopinath case.)

where

$$\Delta\boldsymbol{\lambda}^{\mathbf{s}}_{\mathbf{r\_vm}} = \frac{\hat{L}_r}{\hat{L}_m}\left(\frac{\Delta\mathbf{v_s}}{s^2} - r_s\frac{\Delta\mathbf{i_s}}{s^2} - \sigma L_s\frac{\Delta\mathbf{i_s}}{s}\right)$$

$$\Delta\boldsymbol{\lambda}^{\mathbf{s}}_{\mathbf{r\_cm}} = \hat{r}_r\frac{\hat{L}_m}{\hat{L}_r}\Big/\left(s + \left(\frac{\hat{r}_r}{\hat{L}_r} - j\omega_r\right)\right)\frac{\Delta\mathbf{i_s}}{s}.$$

In the case of the improved Gopinath model flux observer, $\Delta\boldsymbol{\lambda}^{\mathbf{s}}_{\mathbf{r}}$ can be analyzed and solved as shown in (16). In (16), it can be seen that only the effect of the offset current influences the flux estimation as follows:

$$\Delta\boldsymbol{\lambda}^{\mathbf{s}}_{\mathbf{r}} = \left(\hat{r}_r\frac{\hat{L}_m}{\hat{L}_r}\Big/\left(\frac{\hat{r}_r}{\hat{L}_r} - j\omega_r\right)\right)\Delta\mathbf{i_s}. \tag{16}$$

Flux error of the proposed model due to the offset voltage and offset current is identical with the improved Gopinath model. In case of the full- and reduced-order flux observers, the flux error can be analyzed and found as shown in (17) and (18), respectively, as follows:

$$\Delta\boldsymbol{\lambda}^{\mathbf{s}}_{\mathbf{r}} = \frac{C_2}{C_0}\frac{\hat{L}_r}{\hat{L}_m}(\Delta\mathbf{v_s} - r_s\Delta\mathbf{i_s}) + \left(\hat{r}_r\frac{\hat{L}_m}{\hat{L}_r}\Big/\left(\frac{\hat{r}_r}{\hat{L}_r} - j\omega_r\right)\right)\Delta\mathbf{i_s} \tag{17}$$

$$\Delta\boldsymbol{\lambda}^{\mathbf{s}}_{\mathbf{r}} = \frac{C_4}{C_3}\frac{\hat{L}_r}{\hat{L}_m}(\Delta\mathbf{v_s} - r_s\Delta\mathbf{i_s}) + \left(\hat{r}_r\frac{\hat{L}_m}{\hat{L}_r}\Big/\left(\frac{\hat{r}_r}{\hat{L}_r} - j\omega_r\right)\right)\Delta\mathbf{i_s}. \tag{18}$$

The steady-state error due to the offset voltage is zero only in the improved Gopinath model and proposed model, and the flux error due to the offset current exists in all the linear flux observers. The flux error of the full- and reduced-order flux observer can be varied with the selection of the gain matrices. Thus, in these flux observers (full- and reduced-order flux observer), the necessity of accurately measured voltages at low and zero speeds is expected to be a significant limitation for the implementation.

VII. Effects of Parameter Variation

The parameters variation of the induction machine is caused by the various operating conditions, e.g., by ambient temperature, speed, flux level, and even by production to production. The robustness to the parameter variation is requisite for the practical estimation in the flux observer. The FRF is helpful for evaluating sensitivity of the observer to the parameters of the induction machine [2]. The effectiveness of the proposed flux observer can be confirmed through the comparison between the FRF of the improved Gopinath model and that of the proposed model. The FRF of all the linear flux observers can be expressed as follows with the observer characteristic function:

$$\frac{\hat{\boldsymbol{\lambda}}^{\mathbf{s}}_{\mathbf{r}}}{\boldsymbol{\lambda}^{\mathbf{s}}_{\mathbf{r}}} = F(s)\mathbf{FRF_{vm}} + \big(1 - F(s)\big)\mathbf{FRF_{cm}} \tag{19}$$

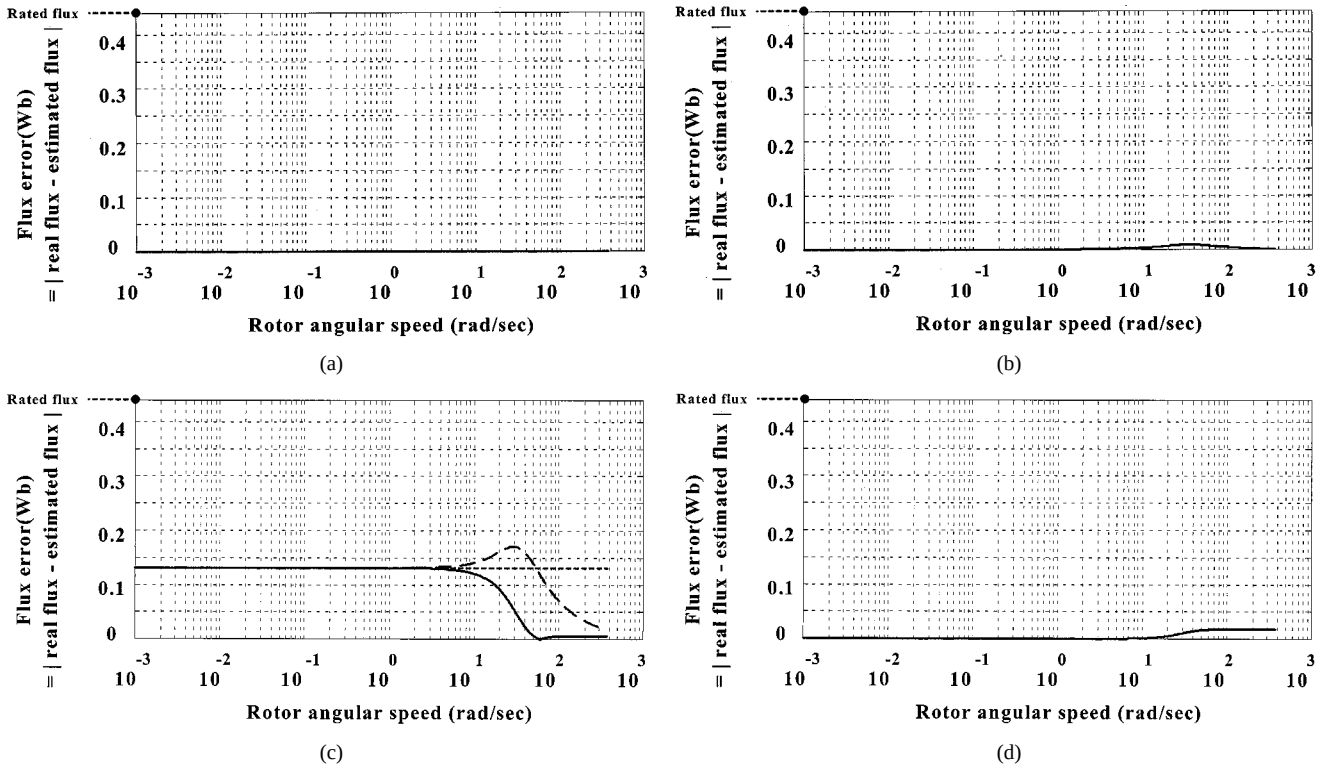

Fig. 9. Numerical analysis: flux errors of the flux observer at no load. (a) $\hat{\boldsymbol{r}}_r = 1.4\boldsymbol{r}_r$ cases. (b) $\hat{r}_s = 1.3r_s$ case. (c) $\hat{L}_m = 0.7L_m$ case (flat dotted line is the flux error of current model). (d) $\hat{\sigma}\hat{L}_s = 1.9\sigma L_s$ cases. (Solid line: proposed case; dotted line: improved Gopinath case.)

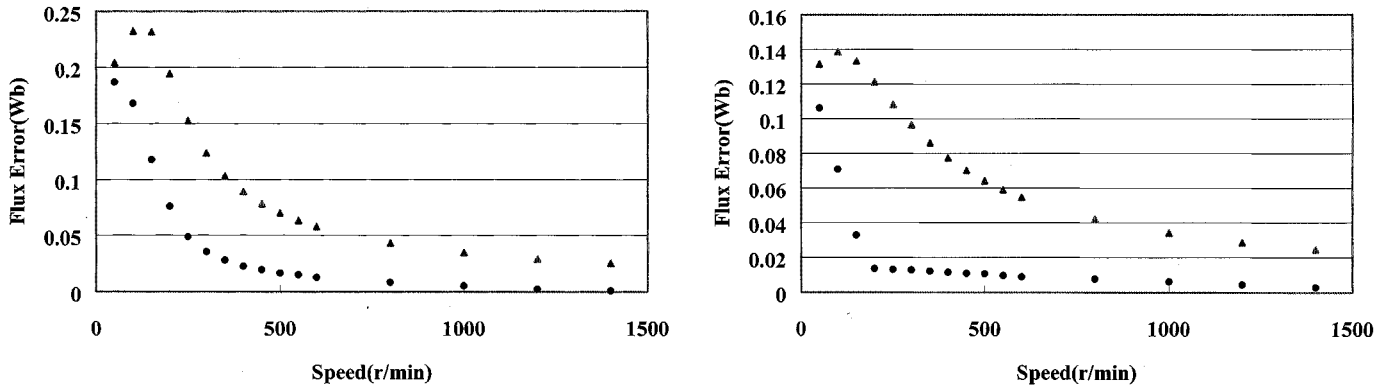

Fig. 10. Experimental results: flux error at stead state. (a) $\hat{L}_m = 0.7L_m$ and no load condition. (b) $\hat{r}_r = 1.4r_r$ and 50% load condition. (Triangular data are flux errors from a detuned case of the improved Gopinath model. Circular data are flux errors from a detuned case of the proposed model.)

where

$$\mathbf{FRF_{vm}} = \frac{\hat{\boldsymbol{\lambda}}_{\mathbf{r\_vm}}}{\boldsymbol{\lambda}_{\mathbf{r\_vm}}} = \frac{\hat{L}_r L_m}{L_r \hat{L}_m}\left(1 + \frac{L_r^2}{r_r L_m^2}\left(\frac{r_r}{L_r} + j\omega_{sl}\right) \cdot \left(\left(\sigma L_s - \hat{\sigma}\hat{L}_s\right) - j\,\frac{r_s - \hat{r}_s}{\omega_e}\right)\right)$$

$$\mathbf{FRF_{cm}} = \frac{\hat{\boldsymbol{\lambda}}_{\mathbf{r\_cm}}}{\boldsymbol{\lambda}_{\mathbf{r\_cm}}} = \frac{\hat{r}_r \hat{L}_m}{r_r L_m}\frac{(j\omega_{sl}L_r + r_r)}{(j\omega_{sl}\hat{L}_r + \hat{r}_r)}.$$

Therefore, the flux error can be described as follows by using the FRF:

$$\left|\boldsymbol{\lambda}_{\mathbf{r}}^{\mathbf{s}} - \hat{\boldsymbol{\lambda}}_{\mathbf{r}}^{\mathbf{s}}\right| = \left|\boldsymbol{\lambda}_{\mathbf{r}}^{\mathbf{s}}\right|\left|1 - \frac{\hat{\boldsymbol{\lambda}}_{\mathbf{r}}^{\mathbf{s}}}{\boldsymbol{\lambda}_{\mathbf{r}}^{\mathbf{s}}}\right| = \left|\boldsymbol{\lambda}_{\mathbf{r}}^{\mathbf{s}}\right|\left|1 - \mathbf{FRF}\right|. \qquad (20)$$

In numerical analysis and experiment, a 22-kW induction machine has been used whose parameters are summarized in Table II. The transition frequency (ω_c) between the current model and voltage model is designed to be the same (6 Hz) in both cases of the improved Gopinath model and the proposed model. In the numerical analysis and experiment, only the result of the improved Gopinath model flux observer compared with that of the proposed flux observer. That is because a similar result will be given with the other flux observers, and the other flux observers have the defects of offset voltage with the voltage model, as explained in Section VI. The estimated flux error (distance between the real flux and estimated flux) due to the parameter (r_r, L_m, r_s, and σL_s) uncertainties are shown in Figs. 8 and 9 where the rated flux is 0.44 Wb.

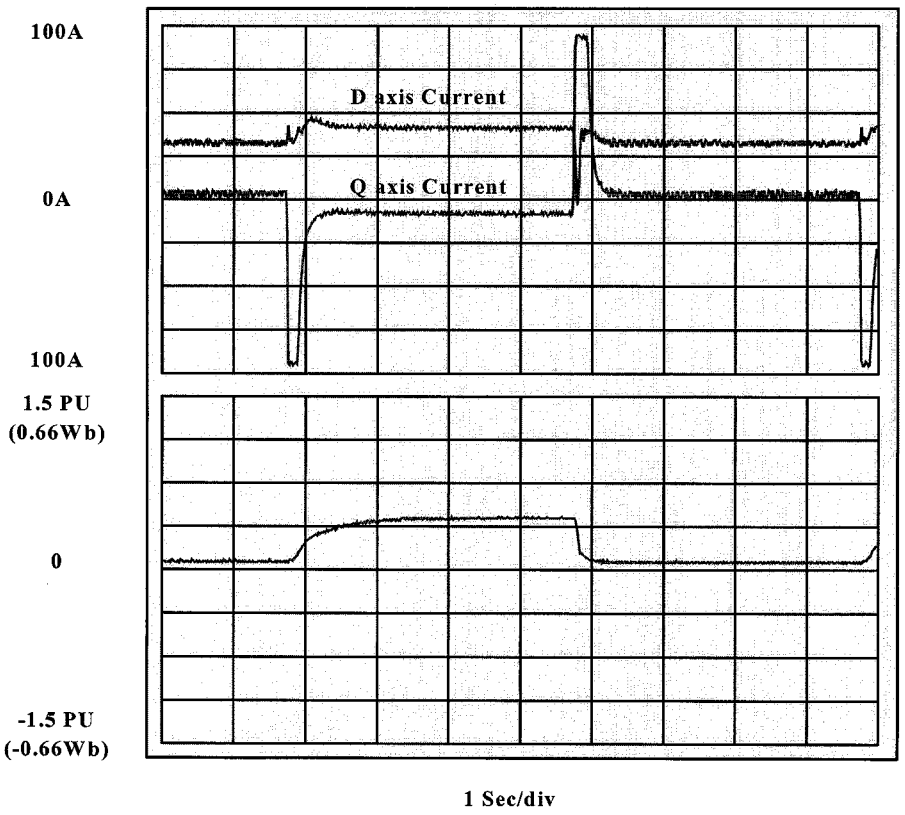

(a)

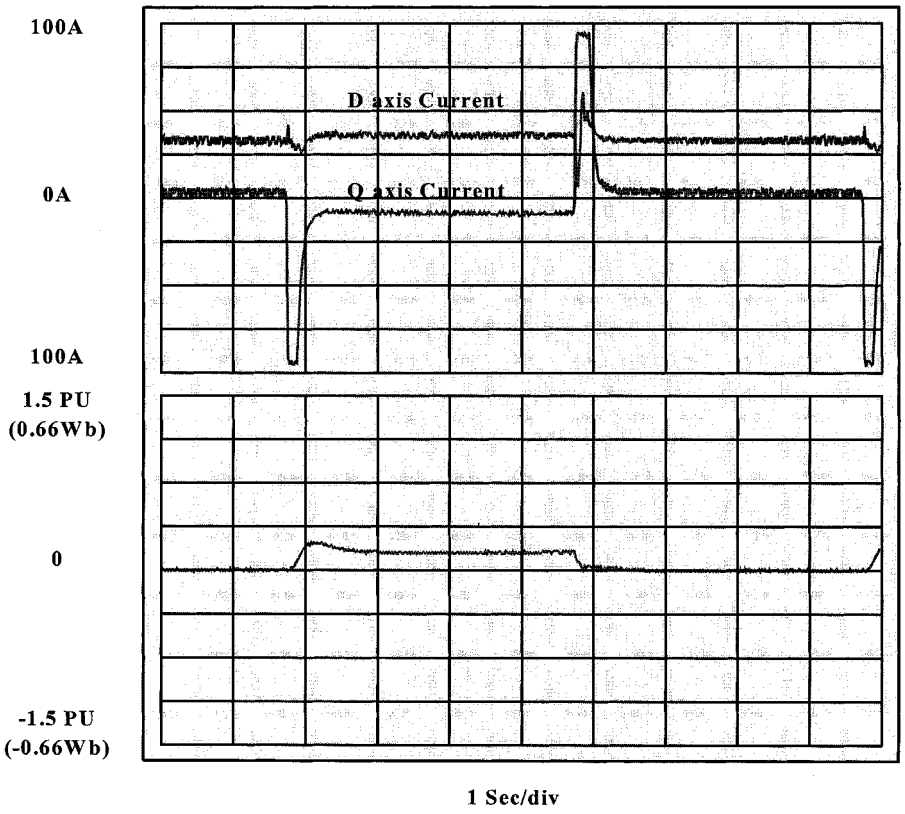

(b)

Fig. 11. Speed control performances with direct field-oriented control: d- and q-axis regulated currents and flux errors ($\hat{L}_m = 0.7L_m$, no load condition, and speed reference step variation between 200–1200 r/min). (a) Characteristics of the improved Gopinath model (detuned case of the improved Gopinath model). (b) Characteristics of the proposed model (detuned cased of the proposed model).

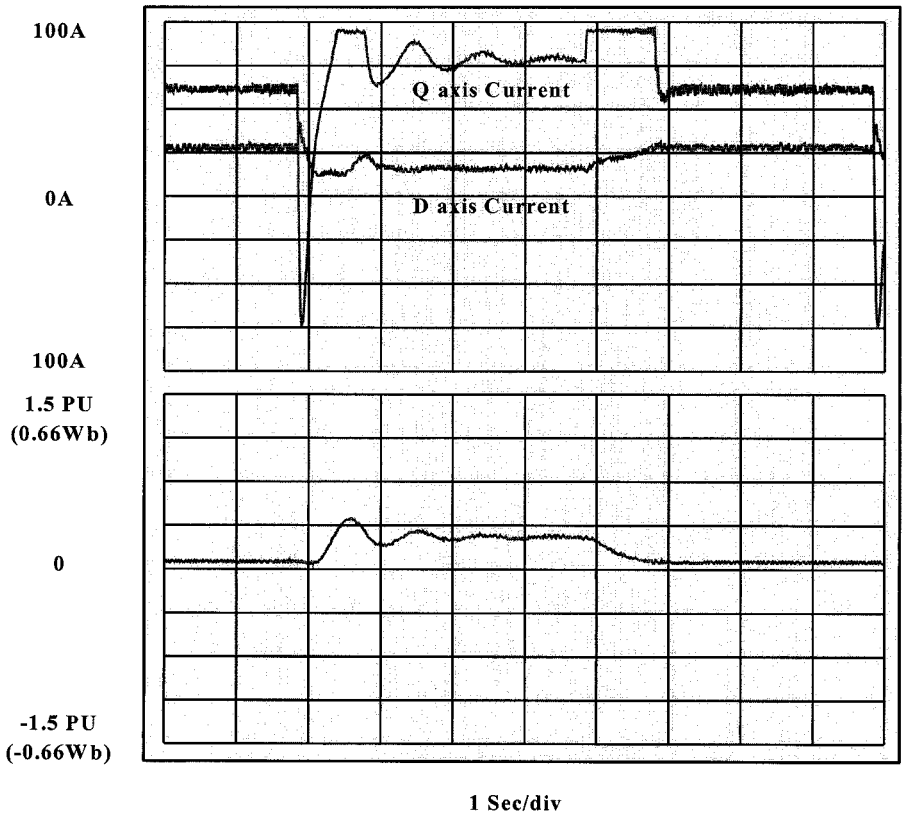

(a)

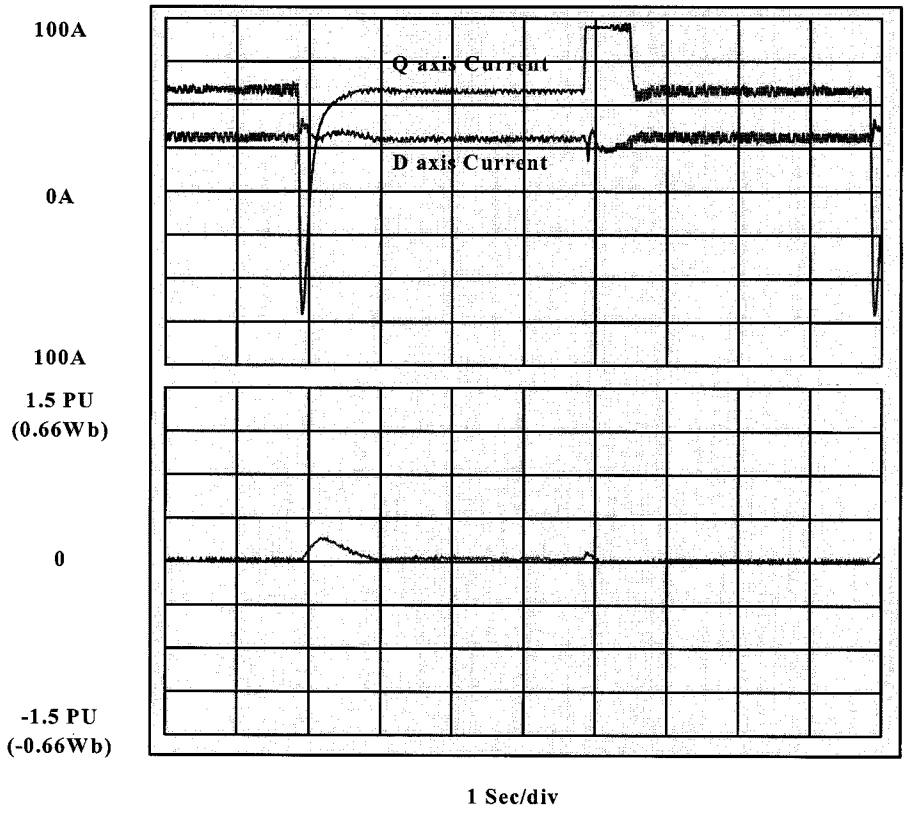

(b)

Fig. 12. Speed control performances with direct field-oriented control: d- and q-axis regulated currents and flux errors ($\hat{r}_r = 1.4r_r$, 50% load condition, and speed reference step variation between 200–1200 r/min). (a) Characteristics of the improved Gopinath model (detuned case of the improved Gopinath model). (b) Characteristics of the proposed model (detuned cased of the proposed model).

$$\frac{s\frac{\hat{L}_m}{\hat{L}_r}\left(\hat{r}_r\frac{\hat{L}_m}{\hat{L}_r}+g_3+jg_4\right)\left(\frac{1}{\sigma\hat{L}_s}\right)}{\left(s+\frac{1}{\sigma\hat{L}_s}\left(\hat{r}_s+\hat{r}_r\frac{\hat{L}_m^2}{\hat{L}_r^2}\right)-g_1-jg_2\right)\left(s+\frac{\hat{r}_r}{\hat{L}_r}-j\omega_r\right)-\frac{\hat{L}_m}{\sigma\hat{L}_s\hat{L}_r}\left(\frac{\hat{r}_r}{\hat{L}_r}-j\omega_r\right)\left(\hat{r}_r\frac{\hat{L}_m}{\hat{L}_r}+g_3+jg_4\right)} \tag{21}$$

Fig. 8 shows the analysis results under the rated slip condition and Fig. 9 under the no load condition. In Fig. 8(a) and (c), as the synchronous speed increases, estimated flux error decreases since the estimated flux converges to the estimated flux from the voltage model. The estimated flux error of the proposed flux observer is much smaller than that of the improved Gopinath model flux observer in detuned cases of r_r and L_m in Fig. 8(a) and (c). Note that, around the transition frequency, the flux error of the improved Gopinath model is larger than that of current model in Fig. 8(a) and (c). In Fig. 8(b) and (d), the estimated flux errors of the proposed flux observer are nearly the same and a little worse compared with those of the improved Gopinath model flux observer in detuned cases of r_s and σL_s because of the relatively fast convergence to the incorrect estimated flux from the voltage model. However, the difference of flux errors due to the detuned case of σL_s is relatively small and the flux error has a similar tendency with the improved Gopinath model as the rotor angular speed increases. Considering that the tuning of r_r and L_m are more difficult than that of r_s and σL_s, the proposed rotor-flux observer is better than the improved Gopinath model in the real application. Additionally, in Fig. 9 at the no load condition, the flux error is mainly caused only by the L_m uncertainty. The estimated flux error of the proposed flux observer is much smaller than that of the improved Gopinath model flux observer in detuned cases of L_m in Fig. 9(c).

VIII. Experimental Results

Various experiments have been carried out. The flux error has been measured by assuming that the real flux can be estimated from the well-tuned improved Gopinath model since the position of the real flux cannot be measured directly. In the experimental setup, the phase currents and rotor angular speed are measured. Figs. 10–12 show experimental results for the purpose of comparison with the improved Gopinath model and the proposed model. In Fig. 10, all the points are obtained under the conditions that the measurement is performed with no variation of speed and load torque. Note that the all flux error points of the proposed model are smaller than those of the improved Gopinath model, such as the numerical analysis results in Section VII. In Figs. 11 and 12, the properties of dynamic and steady state can be evaluated, where the speed control is performed under the conditions that speed reference changes between 200–1200 r/min.

Fig. 11(a) and (b) is obtained under no load conditions ($\hat{L}_m = 0.7L_m$) and Fig. 12(a) and (b) is obtained under the 50% load conditions ($\hat{r}_r = 1.4r_r$). In Figs. 11 and 12, the flux errors of the proposed flux observer are much smaller than those of the improved Gopinath model flux observer in steady state (200 and 1200 r/min) and even in the transient state (both the accelerating and decelerating ranges).

In case of the improved Gopinath model, the speed control nearly failed in the case of Fig. 12(a). Contrary to the improved Gopinath model in Fig. 12(a), the flux error of the proposed model in Fig. 12(b) is nearly zero, except with the decelerating ranges. From these experiments, the validity of the proposed flux observer has been verified.

IX. Conclusion

In this paper, a generalized analysis method called the observer characteristic function method has been proposed to analyze all kinds of linear flux observers in an unified form. With the observer characteristic function, the effects of the voltage and currents offset and the effects of parameter variation have been analyzed. The estimated rotor-flux error involved in the classical methods has also been clarified. A novel rotor-flux observer based on this analysis has been presented. The effectiveness of the proposed observer has been verified by analytic and experimental results.

Appendix

Observer characteristic function of the full-order observer [5] is written as (21), shown at the top of this page.

The observer characteristic function of the reduced-order observer [7] is written as follows:

$$\frac{-s\left((g_{r1}+jg_{r2})\frac{1}{\sigma\hat{L}_s}\right)\frac{\hat{L}_m}{\hat{L}_r}}{\left\{s+(g_{r1}+jg_{r2})\frac{\hat{L}_m}{\sigma\hat{L}_s\hat{L}_r}\left(\frac{\hat{r}_r}{\hat{L}_r}-j\omega_r\right)+\left(\frac{\hat{r}_r}{\hat{L}_r}-j\omega_r\right)\right\}}. \tag{22}$$

References

[1] I. Takahashi and T. Noguchi, "A new quick-response and high-efficiency control strategy of an induction motor," *IEEE Trans. Ind. Applicat.*, vol. IA-22, pp. 820–827, Sept./Oct. 1986.

[2] P. L. Jansen and R. D. Lorenz, "A physically insightful approach to the design and accuracy assessment of flux observers for field oriented induction machine drives," *IEEE Trans. Ind. Applicat.*, vol. 30, pp. 101–110, Jan./Feb. 1994.

[3] P. L. Jansen, R. D. Lorenz, and D. W. Novotny, "Observer-based direct field orientation: Analysis and compensation of alternative methods," *IEEE Trans. Ind. Applicat.*, vol. 30, pp. 945–953, Jul./Aug. 1994.

[4] T. Ohtani, N. Takada, and K. Tanaka, "Vector control of induction motor without shaft encoder," *IEEE Trans. Ind. Applicat.*, vol. 28, pp. 157–164, Jan./Feb. 1992.

[5] H. Kubota, K. Matsuse, and T. Nakano, "DSP-based speed adaptive flux observer of induction motor," *IEEE Trans. Ind. Applicat.*, vol. 29, pp. 344–348, Mar./Apr. 1993.
[6] ——, "New adaptive flux observer of induction motor for wide speed range motor drives," in *IEEE IECON'90*, pp. 921–926.
[7] H. Tajima and Y. Hori, "Speed sensorless field-orientation control of the induction machines," *IEEE Trans. Ind. Applicat.*, vol. 29, pp. 175–180, Jan./Feb. 1993.
[8] G. C. Verghese and S. R. Sanders, "Observers for flux estimation in induction machines," *IEEE Trans. Ind. Electron.*, vol. 35, pp. 85–94, Feb. 1988.

Jang-Hwan Kim (S'02) was born in Kwangju, Korea, in 1975. He received the B.S. and M.S. degrees in electrical engineering from Seoul National University, Seoul, Korea, in 1999 and 2001, respectively, and is currently working toward the Ph.D. degree at Seoul National University.

His research interests are high-performance ac machine drives and electric machines.

Jong-Woo Choi (S'93–M'96) was born in Taegu, Korea, in 1969. He received the B.S., M.S., and Ph.D. degrees in electrical engineering from Seoul National University, Seoul, Korea, in 1991, 1993, and 1996, respectively.

From 1996 to 2000, he was a Research Engineer with the LG Industrial Systems Company. Since 2001, he has been on the faculty of the School of Electronic and Electrical Engineering, Kyungpook National University, Taegu, Korea, where he is currently an Assistant Professor. His research interests are static power conversion and electric machine drives.

Seung-Ki Sul (S'78–M'80–SM'98–F'00) was born in Korea, in 1958. He received the B.S., M.S., and Ph.D. degrees in electrical engineering from Seoul National University, Seoul, Korea, in 1980, 1983, and 1986, respectively.

From 1986 to 1988, he was an Associate Researcher with the Department of Electrical and Computer Engineering, University of Wisconsin–Madison. From 1988 to 1990, he was a Principal Research Engineer with the Gold-Star Industrial Systems Company. Since 1991, he has been a member of the faculty of the School of Electrical Engineering, Seoul National University, where he is currently a Professor. His current research interests are power-electronic control of electric machines, electric vehicle drives, and power-converter circuits.